Journal of Heat and Mass Transfer Research

Journal homepage: http://jhmtr.semnan.ac.ir

Semnan University

Thermodynamic Properties of Monatomic, Diatomic, and Polyatomic Gaseous Natural Refrigerants: A Molecular Dynamics Simulation

Milad Abbasi, Ali Rajabpour *

Advanced Simulation and Computing Laboratory, Mechanical Engineering Department, Imam Khomeini International University, Qazvin,Iran.

PAPER INFO

Paper history:
Received: 2020-09-11
Revised: 2020-12-07
Accepted: 2020-12-09

Keywords:
Natural refrigerants;
Molecular dynamics simulation;
Statistical thermodynamics;
Interatomic potential.

ABSTRACT

Owing to their lower adverse environmental impacts, natural refrigerants have recently attracted a huge deal of attention. In this regard, the present study is aimed to evaluate the thermodynamic properties of different gaseous natural refrigerants at the molecular level using molecular dynamics (MD) simulations. In this context, the density (as a representative of structural features), enthalpy, and specific heat capacity (as representatives of energy properties) of several natural gaseous refrigerants including helium, nitrogen, methane, and ethane were assessed. Lennard-Jones potential was used for simulation of helium and nitrogen while AIREBO potential and OPLS-AA force-fields were employed for simulation of methane and ethane as polyatomic hydrocarbon refrigerants. Simulations are carried out at various temperatures above the boiling point and pressures of 1, 2, and 5 bar. MD results were in good agreement with the experimental data. Among the applied potentials, AIREBO potential offered results closer to the experimental data as compared with OPLS-AA force-field. The methane-ethane mixture was also addressed at different pressures and compared with the Peng-Robinson equation of state. The results of this study indicated that molecular dynamics can be employed as a reliable tool for predicting the thermodynamic properties of natural refrigerants. The results can be used in the refrigeration cycles.

DOI: 10.22075/jhmtr.2020.21350.1305

1. Introduction

Recent years have witnessed the development of new-generations of refrigerants to reduce the overall greenhouse gas emission (Kyoto protocol, 1997) to meet the environmental regulations issued by the European Union (F-gas regulations)[1]. In this regard, new alternative refrigerants with desirable thermodynamics properties, safety, and reliability are highly demanded. Natural refrigerants such as helium, nitrogen, ammonia, hydrocarbons, water, and air have been investigated as new alternative refrigerants due to their promising ozone depletion potential (ODP) and global warming potential (GWP). Although the GWP of some hydrocarbons such as methane is lower than other refrigerants, they offer high GWP values in comparison to CO_2. Hydrocarbons (HC) mainly encompass hydrogen and carbon and can be naturally found in large concentrations in crude oil. Non-toxic hydrocarbons are a new class of refrigerant which have exhibited great promises as an eco-friendly alternative for the CFC/HCFC/HFC fluorocarbons (associated with ozone layer damage). Moreover, owing to their availability and reasonable price, hydrocarbons refrigerants have found extensive applications. Pure hydrocarbons such as methane, ethane, propane, and butane as well as their mixture at different ratios can be mentioned as well-known hydrocarbon refrigerants.

The knowledge of the thermodynamic properties of refrigerants is essential in the design and optimization of thermodynamic systems such as air conditioning systems and the Rankine cycle. These properties can be determined through simulation or experiments. Modeling and simulation techniques based on statistical physics as well as the equation of state (EOS)[2,3] have been widely used to explore the thermodynamics, structural, and transport features of the refrigerants. Some theoretical studies have modeled the thermodynamic properties of pure and mixed

* *Corresponding Author: Ali Rajabpour , Advanced Simulation and Computing Laboratory, Mechanical Engineering Department, Imam Khomeini International University, Qazvin, Iran.*
Email: Rajabpour@eng.ikiu.ac.ir

refrigerants[4–6]. Prediction of the thermodynamic properties of natural refrigerants can be helpful in numerous applications. Although several classical and novel equations of state can reproduce thermodynamic properties with excellent accuracy over a broad range of temperatures and pressures, these models generally fail in providing both volumetric and transport properties using the same framework. This issue could be resolved by a molecular modeling approach[7–10]. In other words, although models such as the Peng-Robinson equation of state can predict thermodynamic properties, computer-based simulation of the thermodynamic properties of refrigerants can determine properties unachievable by the equation of state approaches.

MD method has been extensively employed in various fields including chemistry, biology, physics, and engineering for studying thermodynamic and transport properties of molecular systems from microscopic to macroscopic realms. A successful MD simulation requires an accurate understanding of the interarticular interactions. The MD simulation of gaseous molecules such as helium (He), nitrogen (N_2), and light hydrocarbons has been the subject of a few investigations over the past two decades[11–17]. Tchouar et al used molecular dynamic method to find thermodynamic, structural and transporting properties of liquid helium, neon, methane and nitrogen [18]. Abbaspour employed OPLS-SITE to investigate the pressure of methane as a function of density and used MD simulation to determine a new equation of state for methane[12]. Thermodynamic properties of supercritical CH_4 and CO_2 were also studied in terms of various united and rigid three-body models[19,20]. Moreover, the performance of molecular dynamics simulation was evaluated on a mixture of refrigerants. Some of the refrigerants such as R-436 are a mixture of two or more pure hydrocarbon refrigerants (such as propane and butane). The percentage of each component could significantly influence the thermodynamic properties of the mixture. The Peng-Robinson equation of state is a common approach to calculate the thermodynamic properties of mixed refrigerants. Mafi et al. used the Peng-Robinson equation of state to analyze the mixed refrigerant cycle[21]. Jeong and Alam studied the homogeneous condensation phenomenon of R600a refrigerant in the vapor compression refrigeration system[22]. They computed densities of both phases and investigated the critical time of phase transition in the homogeneous condensation process. Duan et al. examined the evaporation of R32/R1234yf nano-droplets on a smooth substrate and found out when the mole fraction of R32 decreased the extent of evaporation declined[23].

In this paper, to calculate the thermodynamic properties (density, enthalpy, and specific heat) of natural gaseous refrigerants and comparing with experimental data, non-bonded potential (Lennard-Jones) as well as bonded potentials with rigid and flexible bonds (e.g. optimized potential for liquid simulations-all atom (OPLS-AA)[24] and adaptive intermolecular reactive bond order (AIREBO)[25]) were employed. Helium is a monoatomic refrigerant and was simulated by LJ potential. Moreover, LJ potential was applied to nitrogen as a diatomic molecule to obtain its properties and to compare them with experimental data. Then, the OPLS-AA force-field and AIREBO potentials were examined for rigid hydrocarbon molecules (CH_4 and C_2H_6). Finally, a methane-ethane mixture (50% molar fraction) was simulated using AIREBO potential and its density and the enthalpy were calculated and compared with the Peng-Robinson equation of state results as experimental data were not available. Since in many processes of multi-stage refrigeration cycles, refrigerants are also in the gas phase in addition to the liquid phase, the results are also applicable in the cryogenic industry.

2. Simulation details

In this study, all MD simulations are performed using large-scale atomic/molecular parallel simulator (LAMMPS) package[26]. The equations of motion were integrated with the standard Velocity-Varlet[27] algorithm with a time step of 1.0 fs. All intermolecular interactions for hydrocarbons were determined within a cut-off distance of 10.0 Å. The molecular formations used to initialize the simulations were generated utilizing the Moletemplate package[28]. The simulations were carried out using different numbers of molecules located in a cubic box. Periodic boundary conditions were applied along all the three cartesian directions. To equilibrate the system, simulations were run for ~2 ns. Then the simulation was continued for 5 ns to record the desired properties. The temperature and pressure of the system are controlled with the Nośe-Hoover thermostat and barostat. The simulations are divided into five equal intervals and the standard deviations of the intervals were used to estimate the statistical uncertainties.

The pairwise non-bonded interactions between two atoms can be described by the Mie potential[29] :

$$u_{LJ} = f\varepsilon_{ab}\left[\left(\frac{\sigma_{ab}}{r_{ab}}\right)^{t} - \left(\frac{\sigma_{ab}}{r_{ab}}\right)^{z}\right] \quad (1)$$

where u_{LJ} shows the pair-potential energy and r_{ab} represents the distance between the two atoms. Also, ε_{ab} is the maximum potential depth and σ_{ab} denotes the potential length scale. t and z are the repulsive and attractive exponents, respectively. The constant of f is a function of the given exponents, defined as:

$$f = \frac{t}{t-z}\left(\frac{t}{z}\right)^{\frac{z}{t-z}} \quad (2)$$

The Lennard-Jones potential is a particular case of the Mie potential, were t and z are 12 and 6, respectively. It was shown that choosing t=12 and z=6 could properly estimate the properties of He [29][36]. However, it was found that the intermolecular repulsions in He are actually softer than those indicated by an inverse twelfth

power[30]. For hydrocarbon refrigerants, a three-body force-field (OPLS-AA) and a potential (AIREBO) were considered. The general OPLS-AA force-field has the following form:

$$U_{OPLS-AA} = \sum_{strech} k_r (r_{ab} - r_0)^2 + \sum_{bend} k_\theta (\theta_{abc} - \theta_0)^2 + \sum_{j=1}^{N-1} \sum_{i=j+1}^{N} f\left\{\varepsilon_{ab}\left[\left(\frac{\sigma_{ab}}{r_{ab}}\right)^t - \left(\frac{\sigma_{ab}}{r_{ab}}\right)^z\right] + \frac{q_a q_b}{4\pi\varepsilon_0 r_{ab}}\right\} \quad (3)$$

where k_r and k_θ are energy constants, r_0 and r_{ab} are related to the harmonic model for bonds, while θ_0 and θ_{abc} are attributed to the harmonic angle style. Due to high fluctuations[24], intermolecular energy terms representing bond and angle flexibilities (u_{strech} and u_{bend}) were neglected for polyatomic (hydrocarbons) molecules. According to Eq. 3, q_a and q_b are partial charges placed at the center of each atom, and ε_0 shows the vacuum permittivity. The effects of the long-range Columbic and bond interactions can be taken into account through the incorporation of partially changed sites along with the potential model. For interactions between dissimilar atoms, the Lorentz-Berthelot combining rules were used which is usually a part of the original force field. Table 1 represents the coefficients and parameters utilized in the above-mentioned force-field.

3. Results and discussion

This section presents the simulated thermodynamic properties and compares then with experimental data from the national institute of standards and technology (NIST) database[31].

3.1. Helium (a monoatomic refrigerant)

A computational cubic cell (with the size of 20 nm) was constructed including 500 helium atoms as shown in Fig.1. The initial velocity of the atoms was sampled according to Maxwell distribution at desired temperatures.

The density and enthalpy of gaseous helium were computed in the NPT ensemble using a Nośe-Hoover thermostat and barostat at a temperature range of 30 - 200 K and pressures of 1, 2 and 5 bar. The reason for choosing the lower limit is that the Debye temperature of helium is about 29 K; below this temperature, the quantum effects are significant, and classical molecular dynamics is not able to describe it. The results of MD simulations are shown in Fig.2. The density and enthalpy profiles well agree with the NIST data. In the gaseous phase, the maximum absolute deviation (MAD) of the density and the enthalpy between the simulated and NIST data was less than 1%. The heat capacity (C_p) was obtained from the enthalpy-temperature gradient equals to 5.19 $\frac{kJ}{kg.K}$ which is in agreement with the value of $\frac{5}{2}Nk_B$ calculated for an ideal gas, where *N* is the number of He atoms.

Table 1. Coefficients and parameters utilized in two-body potential and three-body force-field. k_B is the Boltzmann constant.

		N-N	He-He	C-C	C-H	H-H
LJ (18 & 21)	σ(Å)	3.31	2.64	3.5	2.93	2.81
	$\frac{\varepsilon}{K_B}$	37.3	10.9	50	20.3	8.6
OPLS-AA	σ(Å)	-	-	3.39	3.08	2.47
	$\frac{\varepsilon}{K_B}$	-	-	55.08	20.6	7.94

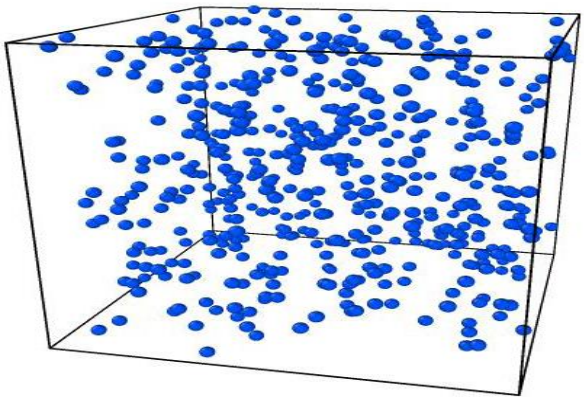

Figure 1. Initial configuration of monoatomic He refrigerant. The size of the cube is 20 nm encompassing 500 He atoms.

3.1. Helium (a monoatomic refrigerant)

A computational cubic cell (with the size of 20 nm) was constructed including 500 helium atoms as shown in Fig.1. The initial velocity of the atoms was sampled according to Maxwell distribution at desired temperatures.

The density and enthalpy of gaseous helium were computed in the NPT ensemble using a Nośe-Hoover thermostat and barostat at a temperature range of 30 - 200 K and pressures of 1, 2 and 5 bar. The reason for choosing the lower limit is that the Debye temperature of helium is about 29 K; below this temperature, the quantum effects are significant, and classical molecular dynamics is not able to describe it. The results of MD simulations are shown in Fig.2. The density and enthalpy profiles well agree with the NIST data. In the gaseous phase, the maximum absolute deviation (MAD) of the density and the enthalpy between the simulated and NIST data was less than 1%. The heat capacity (C_p) was obtained from the enthalpy-temperature gradient equals to 5.19 $\frac{kJ}{kg.K}$ which is in agreement with the value of $\frac{5}{2}Nk_B$ calculated for an ideal gas, where *N* is the number of He atoms.

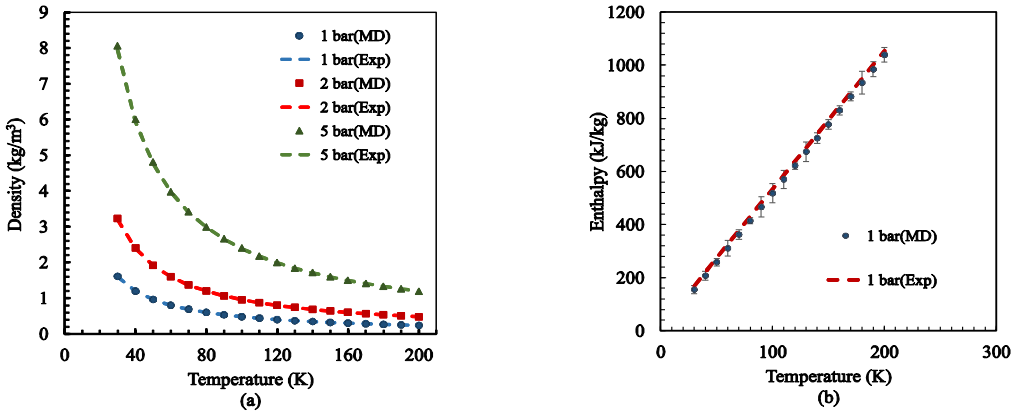

Figure 2. (a) Density and (b) enthalpy diagrams of helium refrigerant at the temperature range of 35 to 200 K and pressures of 1, 2, and 5 bar.

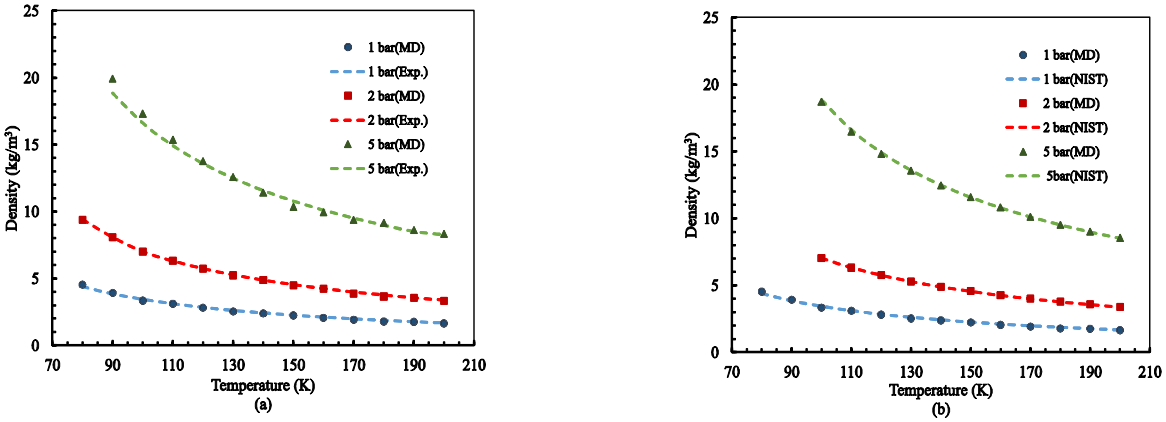

Figure 3. Density diagram of nitrogen refrigerant at the temperature range of 80-200 K and pressures of 1, 2, and 5 bar using (a) rigid and (b) flexible models. Experimental data were taken from NIST[31].

3.2. Nitrogen (a diatomic refrigerant)

Two rigid and flexible models were applied to simulate nitrogen as a diatomic refrigerant.

At first, LJ potential was employed considering rigid bonds and then, the simulation was repeated using flexible harmonic bonds. The dimensions of the simulation box were set at 23 nm. It included 727 nitrogen molecules. Simulations were carried out at the temperatures range of 80-200 K and pressures of 1, 2, and 5 bar. The diagram of density simulated by rigid and flexible models is depicted in Fig.3. Moreover, the enthalpy diagram at P = 1 bar is shown in Fig.4 for both models.

Comparing the simulation results with the NIST data, it is found that the rigid model could better predict the enthalpy rather than the flexible one. However, there is a less than 1% difference between density results obtained from rigid and flexible models. In the range of temperature which is used in the simulation, the behavior of nitrogen is close to ideal gas that can be reason that results of the rigid model have better prediction rather than flexible model. Similar to helium, the heat capacity at constant

Table 2. Coefficients and parameters utilized in two-body potential and three-body force-field. k_B is the Boltzmann constant.

Maximum absolute deviation at the range of 80-200 K				
Property	**Density (%)**			**Enthalpy (%)**
Pressure	1 bar	2 bar	5 bar	1 bar
LJ potential with rigid bond	0.6	0.92	3.2	1.8
LJ potential with flexible bond	0.55	0.8	1.3	23

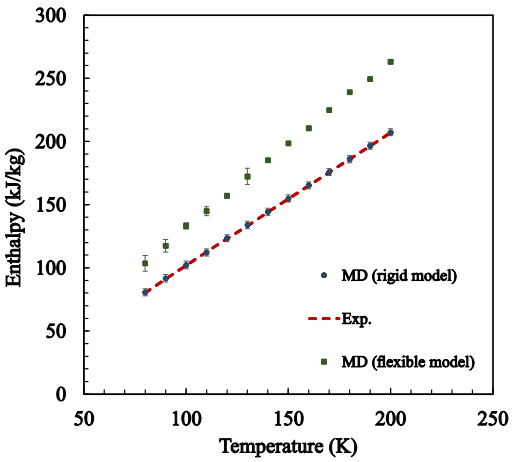

Figure 4. Enthalpy diagram of nitrogen at the temperature range of 80-200 K and P = 1 bar for rigid and flexible models. Experimental data were taken from NIST[31].

pressure for nitrogen was calculated from the enthalpy-temperature diagram as 1.09 $\frac{kJ}{kg \cdot K \cdot}$ for the rigid model showing less than 4% deviation from $\frac{7}{2}Nk_B$ obtained from the ideal gas model. The maximum absolute deviation of density and enthalpy between simulations and experimental data are reported in Table 2.

3. Methane and ethane (polyatomic refrigerants)

Methane and ethane were simulated as polyatomic refrigerants. For both of these refrigerants, the initial dimensions of the simulation box were set to 103 nm encompassing 1000 molecules as shown in Fig.5.

The simulation temperature varied between 200 and 300 K and the pressures of 1, 2, and 5 bar were applied.

Simulations were performed with AIREBO potential and OPLS-AA force-field. For methane, the density and the enthalpy diagram were illustrated in Fig. 6. Both AIREBO and OPLS-AA models could predict the density and the enthalpy with proper accuracy compared to NIST results. The maximum absolute deviation for AIREBO potential and OPLS-AA was 0.65% and 0.8%, respectively. The density and enthalpy diagrams of ethane are shown in Fig.7. It can be seen that the deviation of enthalpy results increased with incrementing the temperature. Moreover, the deviation of ethane was greater than methane. This can be attributed to more vibrational degrees of freedom in ethane rather than methane. The difference in the deviations from experimental data for the two studied compounds can be assigned to several reasons other than the molecular structure. In this case, the force field modeling itself could be a potential reason. The maximum absolute deviation of density and enthalpy between simulations and NIST data are presented in Table 3.

3.4. Methane-ethane mixture

In this section a mixture of methane and ethane with equal molar ratios (50%) was simulated.

The total number of molecules was N=1000. As found in the previous section, AIREBO potential performed better than OPLS-AA force-field in the enthalpy prediction. Thus, AIREBO potential was employed for simulation of the methane-ethane mixture. The studied temperature range was 300-400 K and the pressure values were set to 1, 2, and 5 bar. The density and the enthalpy were calculated and compared with the results of the Peng-Robinson equation of state as shown in Fig. 8. It can be seen that by increasing the temperature, the MD-calculated

Table 3. Maximum absolute deviation of MD-calculated density and enthalpy (AIREBO and OPLS-AA models) from the experimental data from NIST for methane and ethane.

Maximum absolute deviation at the range of 200-300 K(%)					
Property		**Density**			**Enthalpy**
Pressure		**1 bar**	**2 bar**	**5 bar**	**1 bar**
Methane (CH_4)	AIREBO	2.6	1.3	0.7	0.85
	OPLS-AA	3.2	3.34	2.4	1.1
Ethane (C_2H_6)	AIREBO	1.43	1.03	0.82	2.4
	OPLS-AA	2.12	2.2	1.8	7.4

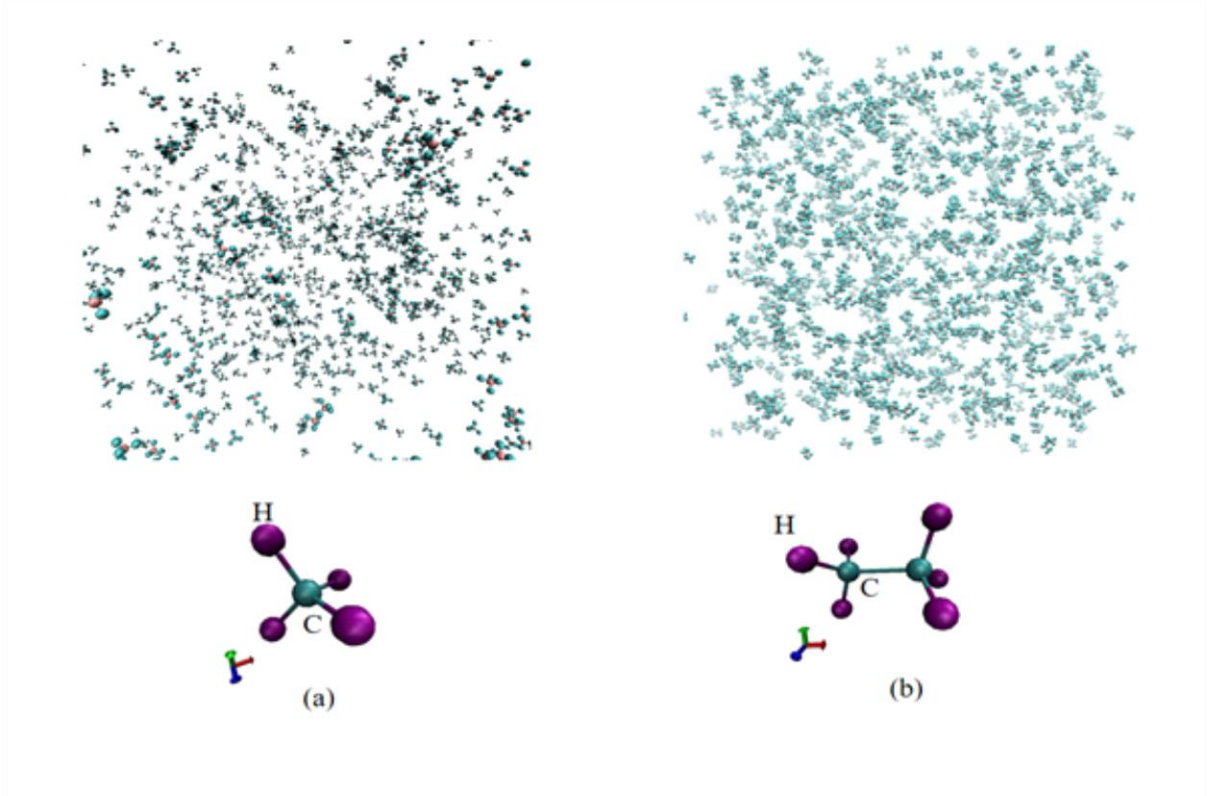

Figure 5. Initial setup of MD simulation for (a) methane and (b) ethane.

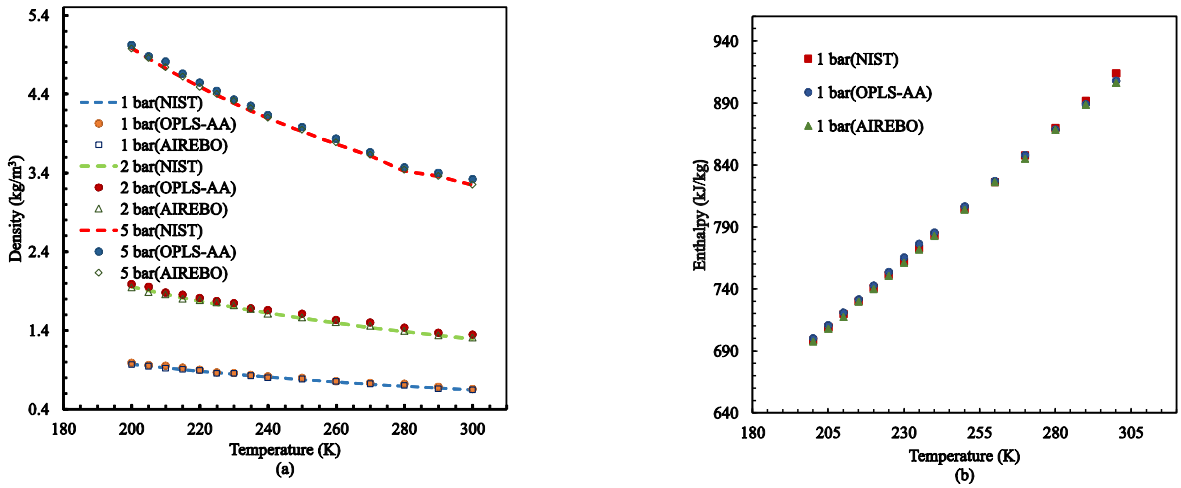

Figure 6. (a) Density diagram of methane refrigerant at the temperature range of 200-300 K and pressures of 1, 2, and 5 bar using AIREBO potential and OPLS-AA force-field. (b) Enthalpy diagram of methane at the temperature range of 200-300 K and p=1 bar using AIREBO potential and OPLS-AA force-field.

enthalpy values deviated from those obtained by the Peng-Robinson equation of state. This discrepancy may be due to either the assumptions used in the Peng-Robinson equation of state or the uncertainties in the coefficients of the AIREBO potential function. However, the difference was less than 4% at 400 K and decreased by reducing the temperature.

Conclusion

MD simulations were carried out using various potentials and force-fields to investigate the thermodynamic properties of pure and mixed refrigerants in the gaseous phase temperature range. The following conclusions can be drawn from the present study:

- LJ potential was used for simulating helium as a monoatomic refrigerant at various temperature and pressure ranges. The calculated densities and

enthalpies were in good agreement with the NIST data. The heat capacity at constant pressure was obtained 5.19 $\frac{kJ}{(kg \cdot K)}$ showing proper agreement with the ideal gas model.

- Two rigid and flexible models were used for simulating nitrogen as a diatomic refrigerant. Despite the similar density prediction of both models, the rigid model outperformed the OPLS-AA forcefield in the case of enthalpy and the heat capacity. The heat capacity at constant pressure was determined 1.09 $\frac{kJ}{(kg \cdot K)}$ exhibiting less than 5% deviation from the ideal gas.
- Methane and ethane were simulated using AIREBO potential and OPLS-AA forcefield at the temperature range of 200-300K. It can be concluded that AIREBO offered a better prediction of enthalpy rather than OPLS-AA for the gaseous phase of hydrocarbon molecules. Moreover, by increasing the mass of the hydrocarbons molecules, the enthalpy results deviated from the experimental data which can be assigned to more sensitivity of enthalpy to the potential parameters as well as more vibrational degrees of freedom.
- Thermodynamic properties of the methane-ethane mixture were also calculated and compared with the results obtained by Peng-Robinson equation of state.
- The enthalpy exhibited considerably more sensitivity to potential parameters as compared with the density which got more intensified at high pressures.

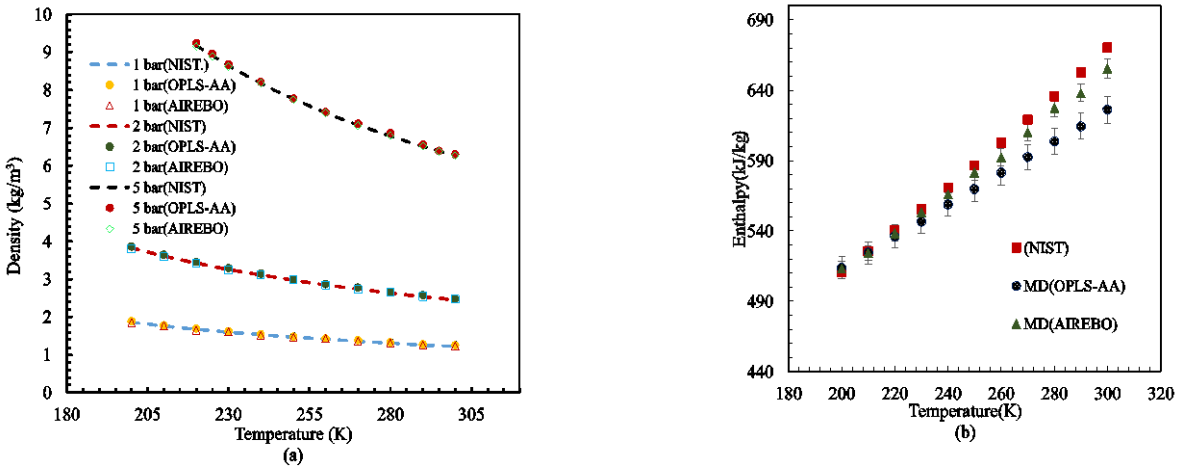

Figure 7. (a) Density diagram of ethane refrigerant at the temperature range of 200-300 K and pressures of 1, 2, and 5 bar using AIREBO potential and OPLS-AA force-field. (b) Enthalpy diagram of methane at the temperature range of 200-300 K and P=1 bar using AIREBO potential and OPLS-AA force-field.

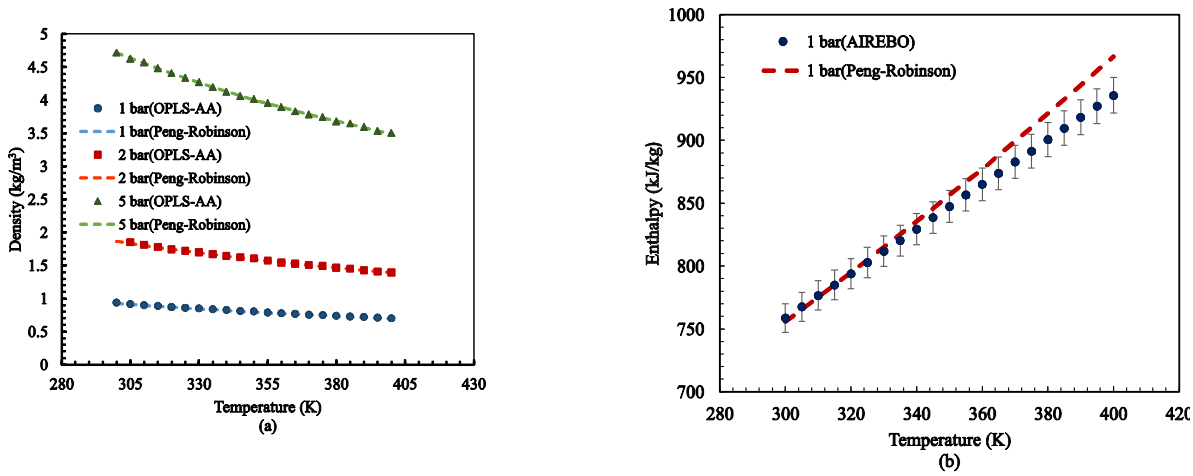

Figure 8. (a) Density diagram of the methane-ethane mixture at T=300-400 K and P =1, 2, and 5 bar using AIREBO potential, (b) the enthalpy diagram at T = 35-200 K and P = 1 bar.

References

[1] S. Barrault, M. Nemer, La F-GasII et son impact sur les émissions de fluides frigorigènes en France à l'Horizon 2035, Refrig. Sci. Technol. (2015) 2412–2419. https://doi.org/10.18462/iir.icr.2015.0058.

[2] B.I. Lee, M.G. Kesler, A generalized thermodynamic correlation based on three-parameter corresponding states, AIChE J. 21 (1975) 510–527. https://doi.org/10.1002/aic.690210313.

[3] D.Y. Peng, D.B. Robinson, A New Two-Constant Equation of State, Ind. Eng. Chem. Fundam. 15 (1976) 59–64. https://doi.org/10.1021/i160057a011.

[4] H. Atalay, M.T. Coban, Modeling of Thermodynamic Properties for Pure Refrigerants and Refrigerant Mixtures by Using the Helmholtz Equation of State and Cubic Spline Curve Fitting Method, Univers. J. Mech. Eng. 3 (2015) 229–251. https://doi.org/10.13189/ujme.2015.030604.

[5] M.O. McLinden, E.W. Lemmon, R.T. Jacobsen, Thermodynamic properties for the alternative refrigerants, Int. J. Refrig. 21 (1998) 322–338. https://doi.org/10.1016/S0140-7007(97)00081-9.

[6] C. Coquelet, J. El Abbadi, C. Houriez, Prévision des propriétés thermodynamiques des fluides frigorigènes avec une nouvelle équation cubique d'état à trois paramètres, Int. J. Refrig. 69 (2016) 418–436. https://doi.org/10.1016/j.ijrefrig.2016.05.017.

[7] P. Strąk, S. Krukowski, Molecular nitrogen-N2 properties: The intermolecular potential and the equation of state, J. Chem. Phys. 126 (2007). https://doi.org/10.1063/1.2733651.

[8] C.G. Aimoli, E.J. Maginn, C.R.A. Abreu, Transport properties of carbon dioxide and methane from molecular dynamics simulations, J. Chem. Phys. 141 (2014). https://doi.org/10.1063/1.4896538.

[9] U.K. Deiters, R.J. Sadus, Ab Initio Interatomic Potentials and the Classical Molecular Simulation Prediction of the Thermophysical Properties of Helium, J. Phys. Chem. B. 124 (2020) 2268–2276. https://doi.org/10.1021/acs.jpcb.9b11108.

[10] M.R. Shirts, J.D. Chodera, Statistically optimal analysis of samples from multiple equilibrium states, J. Chem. Phys. 129 (2008). https://doi.org/10.1063/1.2978177.

[11] E.K. Goharshadi, M. Abbaspour, Determination of potential energy function of methane via the inversion of reduced viscosity collision integrals at zero pressure, Fluid Phase Equilib. 212 (2003) 53–65. https://doi.org/10.1016/S0378-3812(03)00262-0.

[12] M. Abbaspour, Computation of some thermodynamics, transport, structural properties, and new equation of state for fluid methane using two-body and three-body intermolecular potentials from molecular dynamics simulation, J. Mol. Liq. 161 (2011) 30–35. https://doi.org/10.1016/j.molliq.2011.04.002.

[13] S. MURAD, K.E. GUBBINS, Molecular Dynamics Simulation of Methane Using a Singularity-Free Algorithm, in: 1978: pp. 62–71. https://doi.org/10.1021/bk-1978-0086.ch005.

[14] M. Schoen, C. Hoheisel, O. Beyer, Liquid CH4, liquid CF4 and the partially miscible liquid mixture CH4/CF4: A molecular dynamics study based on both a spherically symmetric and a four-centre lennard-jones potential model, Mol. Phys. 58 (1986) 699–709. https://doi.org/10.1080/00268978600101511.

[15] H. Stassen, On the pair potential in dense fluid methane, J. Mol. Struct. THEOCHEM. 464 (1999) 107–119. https://doi.org/10.1016/S0166-1280(98)00540-5.

[16] R.L. Rowley, T. Pakkanen, Determination of a methane intermolecular potential model for use in molecular simulations from ab initio calculations, J. Chem. Phys. 110 (1999) 3368–3377. https://doi.org/10.1063/1.478203.

[17] E.A. Mason, W.E. Rice, The intermolecular potentials of helium and hydrogen, J. Chem. Phys. 22 (1954) 522–535. https://doi.org/10.1063/1.1740100.

[18] N. Tchouar, M. Benyettou, F.O. Kadour, Thermodynamic, Structural and Transport Properties of Lennard-Jones Liquid Systems. A Molecular Dynamics Simulations of Liquid Helium, Neon, Methane and Nitrogen, Int. J. Mol. Sci. 4 (2003) 595–606. www.mdpi.org/ijms/.

[19] T. Kristóf, G. Rutkai, L. Merényi, J. Liszi, Molecular simulation of the Joule-Thomson inversion curve of hydrogen sulphide, Mol. Phys. 103 (2005) 537–545. https://doi.org/10.1080/00268970413331319263.

[20] C.G. Aimoli, E.J. Maginn, C.R.A. Abreu, Force field comparison and thermodynamic

property calculation of supercritical CO2 and CH4 using molecular dynamics simulations, Fluid Phase Equilib. 368 (2014) 80–90. https://doi.org/10.1016/j.fluid.2014.02.001.

[21] M. Mafi, M. Amidpour, S.M.M. Naeynian, Comparison of low temperature mixed refrigerant cycles for separation systems, Int. J. Energy Res. 33 (2009) 358–377. https://doi.org/10.1002/er.1480.

[22] M.S. Alam, J.H. Jeong, Molecular dynamics simulations on homogeneous condensation of R600a refrigerant, J. Mol. Liq. 261 (2018) 492–502. https://doi.org/10.1016/j.molliq.2018.04.022.

[23] X. Wu, Z. Yang, Y. Duan, Evaporation of R32/R1234yf mixture nanodroplets on a smooth substrate: Molecular dynamics simulation, Chem. Phys. Lett. 733 (2019) 136672. https://doi.org/10.1016/j.cplett.2019.136672.

[24] G.A. Kaminski, R.A. Friesner, J. Tirado-Rives, W.L. Jorgensen, Evaluation and reparametrization of the OPLS-AA force field for proteins via comparison with accurate quantum chemical calculations on peptides, J. Phys. Chem. B. 105 (2001) 6474–6487. https://doi.org/10.1021/jp003919d.

[25] S.J. Stuart, A.B. Tutein, J.A. Harrison, A reactive potential for hydrocarbons with intermolecular interactions, J. Chem. Phys. 112 (2000) 6472–6486. https://doi.org/10.1063/1.481208.

[26] S. Plimpton, Fast Parallel Algorithms for Short-Range Molecular Dynamics, J. Comput. Phys. 117 (1995) 1–19. https://doi.org/10.1006/jcph.1995.1039.

[27] L. Verlet, Computer “experiments” on classical fluids. I. Thermodynamical properties of Lennard-Jones molecules, Phys. Rev. 159 (1967) 98–103. https://doi.org/10.1103/PhysRev.159.98.

[28] A.I. Jewett, Z. Zhuang, J.-E. Shea, Moltemplate a Coarse-Grained Model Assembly Tool, 2013. https://doi.org/10.1016/j.bpj.2012.11.953.

[29] On the determination of molecular fields. — II. From the equation of state of a gas, Proc. R. Soc. London. Ser. A, Contain. Pap. a Math. Phys. Character. 106 (1924) 463–477. https://doi.org/10.1098/rspa.1924.0082.

[30] R.K. Pathria, P.D. Beale, Statistical Mechanics, 2011. https://doi.org/10.1016/C2009-0-62310-2.

[31] P.J. Linstrom, W.G. Mallard, The NIST Chemistry WebBook: A chemical data resource on the Internet, J. Chem. Eng. Data. 46 (2001) 1059–1063. https://doi.org/10.1021/je000236i.